5

# Nonlinear Evapotranspiration Modeling Using MLP-NNM and SVM-NNM Approach

Sungwon Kim and Hung Soo Kim
*Dongyang University and Inha University*
*Republic of Korea*

## 1. Introduction

Evapotranspiration (ET) is the sum of volume of water used by vegetaion, evaporated from the soil, and intercepted precipitation (Singh, 1988). ET plays an important role in our environment at global, regional, and local scales. Water entering the evaporation phase of the hydrological cycle becomes unavailable and cannot be recovered for further use (Brutsaert, 1982). In many areas where water resources are scarce, the calculation of this loss becomes imperative in the planning and management of irrigation practices (Kisi, 2007). Evaporation and transpiration occur simultaneously and there is no easy way of distinguishing between the two processes (Allen et al., 1998). Transpiration consists of vaporization of liquid water contained in plant tissues and the vapor removal to the atmosphere. Evaporation occurs at the topsoil if the water is available. When the crop is small, water is predominantly lost by soil evaporation. Once the crop, however, is well developed and completely covers the soil, transpiration becomes the main process.

ET is one of the hydrologic cycle components and the accurate estimation of ET is very important for the researches such as water balance, irrigation design and management, crop yield modeling, and water resources planning and management (Kumar et al., 2002). ET is observed using a lysimeter directly or can be estimated using the water balance method or the climatic variables indirectly. Because the measurements of ET using a lysimeter directly, however, requires much unnecessary time and needs correct and careful experience, it is not always possible in field measurements. Thus, an empirical approach based on the climatic variables is generally used to estimate the ET (Penman, 1948; Allen et al., 1989). In the early 1970s, the Food and Agricultural Organization of the United Nations (FAO), Rome, developed practical procedures to estimate the crop water requirements (Doorenbos & Pruitt, 1977), which have become the widely accepted standard for irrigation studies. A common practice for estimating the ET from a well-watered agricultural crop is to estimate the reference crop ET such as the grass reference evapotranspiration (ETo) or the alfalfa reference evapotranspiration (ETr) from a standard surface and to apply an appropriate empirical crop coefficient, which accounts for the difference between the standard surface and the crop ET.

The emergence of neural networks model has provided many promising results in the field of hydrology and water resources modeling. Due to the ease of application and simple architecture, the neural networks model has become a promising research field with surprising potential. A comprehensive review of the application of neural networks model

to hydrology can be found in ASCE (2000). The success using the neural networks model in many fields of science and engineering suggests that the neural networks model may prove be an effective and efficient way for the modeling of ET process. Recently, the outstanding results using the neural networks model in the fields of ET modeling have been obtained (Sudheer et al., 2003; Trajkovic et al., 2003; Trajkovic, 2005; Kisi, 2006; Kisi, 2007; Jain et al., 2008; Kim & Kim, 2008; Kumar et al., 2008; Landeres et al., 2008; Zanetti et al., 2008; Kumar et al., 2009). Kumar et al. (2002) developed the neural networks models to estimate the daily ETo. They used proper combinations of the observed climatic variables such as solar radiation, temperature, relative humidity, and wind speed for the neural networks models. Kisi & Ozturk (2007) used the neuro-fuzzy models to estimate the FAO-56 PM ETo using the observed climatic variables. They used proper combinations of the observed climatic variables such as air temperature, solar radiation, wind speed, and relative humidity for the neuro-fuzzy models. Kisi (2008) investigated the potential of different neural networks models in the ET modeling. He used proper combinations of the observed climatic variables such as solar radiation, mean temperature, mean relative humidity, and wind speed for the neural networks models. Traore et al. (2010) developed the neural network models to calculate the reference ET complex process in Sudano-Sahelian zone. They proper combinations of the observed climatic variables such as minimum temperature, maximum temperature, extraterrestrial radiation, relative humidity, and wind speed for the neural networks models.

This paper investigates the modeling of FAO-56 PM ETo using the neural networks models. The major objective of the study is to evaluate the potential of neural networks models for estimating the FAO-56 PM ETo using climatic data avaliable. A comparative evaluation of multiple linear regression model (MLRM) and neural networks models including multilayer perceptron neural netwprks model (MLP-NNM) and support vector machine neural networks model (SVM-NNM) are carried out. From this study, we evaluate the impact of MLP-NNM and SVM-NNM performances for the modeling of FAO-56 PM ETo. The optimal MLP-NNM and SVM-NNM can estimate the FAO-56 PM ETo with the least cost and endeavor. Finally, the FAO-56 PM ETo data can be constructed to provide the fundamental data for the drought analysis and irrigation networks systems, Republic of Korea.

## 2. Grass reference evapotranspiration model : FAO-56 PM ETo equation

Penman (1948) combination method links evaporation dynamics with the flux of net radiation and aerodynamic transport characteristics of the natural surface. Based on the observations that latent heat transfer in plant stem is influenced not only by these abiotic factors, Monteith (1965) introduced a surface conductance term that accounted for the response of leaf stomata to its hydrologic environment. This modified form of the Penman-Monteith (PM) ET model. Jensen et al. (1990) measured the ET using the lysimeters at 11 stations located in the different climatic zones of various regions around the world. They compared the results of the lysimeters with those of 20 different empirical equations and methodologies for the ET measurements. It was found that PM ET model showed the optimal results over all the climatic zones. If the observed/measured data for the ET does not exist, therefore, PM ET model can be considered as a standard methodology to estimate the ET. In 8 meteorological stations which were selected for this study, there are no observed data for the grass reference ET (ETo). The data calculated using PM ETo model can be assumed as the observed ETo, whose reliability was verified by many previous studies.

All calculation precedures as used in PM ETo model are based on the FAO guidelines as laid down in the publication No. 56 of the Irrigation and Drainage Series of FAO "Crop Evapotranspiration – Guidelines for Computing Crop Water Requirements" (1998). Therefore, FAO-56 PM ETo equation means the PM ETo equation suggested by the Irrigation and Drainage Paper No.56, FAO. FAO-56 PM ETo equation is given by Allen et al. (1998) and can be shown as the following equation (1).

$$\text{FAO-56 PM ETo} = \frac{0.408\Delta(R_n - G) + \gamma(900/(T+273))u_2(e_s - e_a)}{\Delta + \gamma(1 + 0.34u_2)} \quad (1)$$

where FAO-56 PM ETo = the grass reference evapotranspiration (mm/day); $R_n$ = the net radiation at the crop surface (MJ/m²·day); G = the soil heat flux density (MJ/m²·day); T = the mean daily air temperature at 2m height (˚C); $u_2$ = the wind speed at 2m height (m/sec); $e_s$ = the saturation vapor pressure (kPa); $e_a$ = the actual vapor pressure (kPa); $e_s$ - $e_a$ = the saturation vapor pressure deficit (kPa); Δ = the slope vapor pressure curve (kPa/◦C); and γ = the psychometric constant (kPa/◦C). FAO CROPWAT 8.0 computer program has been used to calculate FAO-56 PM ETo and extraterrestrial radiation ($R_a$). FAO CROPWAT 8.0 computer program allows the user to enter the climatic data available including maximum temperature ($T_{max}$), minimum temperature ($T_{min}$), mean relative hymidity ($RH_{mean}$), mean wind speed ($U_{mean}$), and sunshine duration (SD) for calculating FAO-56 PM ETo. On the base of climatic data available, FAO CROPWAT 8.0 computer program estimates the solar radiation reaching soil surface. Fig. 1(a)-(b) show the calculation of FAO-56 PM ETo using FAO CROPWAT 8.0 computer program in Gunsan and Haenam stations, respectively.

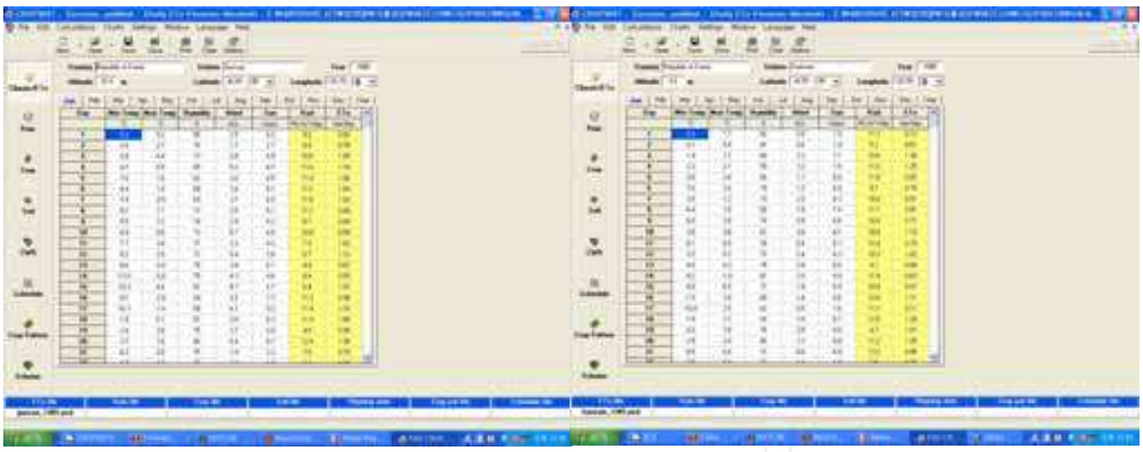

(a) Gunsan station (b) Haenam station

Fig. 1. Calculation of FAO-56 PM ETo using FAO CROPWAT 8.0

## 3. Neural networks models

### 3.1 MultiLayer perceptron neural networks model (MLP-NNM)

MLP-NNM has an input layer, an output layer, and one or more hidden layers between the input and output layers. Each of the nodes in a layer is connected to all the nodes of the next layer, and the nodes in one layer are connected only to the nodes of the immediate next layer. The strength of signal passing from one node to the other depends on the connection

weights of the interconnections. The hidden layers enhance the network's ability to model complex functions. MLP-NNM is trained using the many kinds of backpropagation algorithms. Training performance is a process of adjusting the connection weights and biases so that its output can match the desired output best. Specifically, at each setting of the connection weights, it is possible to calculate the error committed by the networks simply by taking the difference between the desired and actual responses (Simpson, 1990; Specht, 1991; Gallant, 1993; Wasserman, 1933; Bishop, 1995; Tsoukalas & Uhrig, 1997; Haykin, 2009). In this study, MLP-NNM is trained with the Quickprop backpropagation algorithm (BPA). The QuickProp BPA is a training method that operates much faster in the batch mode than the conventional BPA. It has the additional advantage that it is not sensitive to the learning rate and the momentum. In MLP-NNM with five input nodes, the results of the output layer can be written as equation (2).

$$\text{FAO-56 PM ETo} = \Phi_2\left(\sum_{k=1}^{1} W_{kj} \cdot \Phi_1\left(\sum_{j=1}^{5} W_{ji} \cdot X(t) + B_1\right) + B_2\right) \tag{2}$$

where i, j, k = the input layer, the hidden layer, and the output layer, respectively; FAO-56 PM ETo = the grass reference evapotranspiration (mm/day); $\Phi_1(\cdot)$ = the linear sigmoid transfer function of the hidden layer; $\Phi_2(\cdot)$ = the linear sigmoid transfer function of the output layer; $W_{kj}$ = the connection weights between hidden and output layers; $W_{ji}$ = the connection weights between input and hidden layers; $X(t)$ = the time series data of input nodes including mean wind speed ($U_{mean}$), mean temperature ($T_{mean}$), sunshine duration (SD), mean relative humidity ($RH_{mean}$), and max temperature ($T_{max}$); $B_1$ = the bias in the hidden layer; and $B_2$ = the bias in the output layer. A number of MLP-NNM computer programs are now available. NeuroSolutions 5.0 computer program was used to develop MLP-NNM structure. Fig. 2 shows the developed structure of MLP-NNM with five input nodes. Table 1 shows the conditions of training performance for MLP-NNM.

| Index | Assigned Value |
|---|---|
| Stepsize | 1.0 |
| Momentum | 0.5 |
| Maximum Iterations | 50000 |
| Training Threshold | 0.001 |

Table 1. Conditions of training performance for MLP-NNM

### 3.2 Support vector machine neural networks model (SVM-NNM)

SVM-NNM has found wide application in several areas including pattern recognition, regression, multimedia, bio-informatics and artificial intelligence. Very recently, SVM-NNM is gaining recognition in hydrology (Dibike et al., 2001; Khadam & Kaluarachchi, 2004). SVM-NNM implements the structural risk minimization principle which attempts to minimize an upper bound on the generalization error by striking a right balance between the training performance error and the capacity of machine. The solution of traditional neural networks models including MLP-NNM may tend to fall into a local optimal solution, whereas global optimum solution is guaranteed for SVM-NNM (Haykin, 2009). SVM-NNM is a new kind of classifier that is motivated by two concepts. First, transforming data into a high-dimensional space can transform complex problems into simpler problems that can use

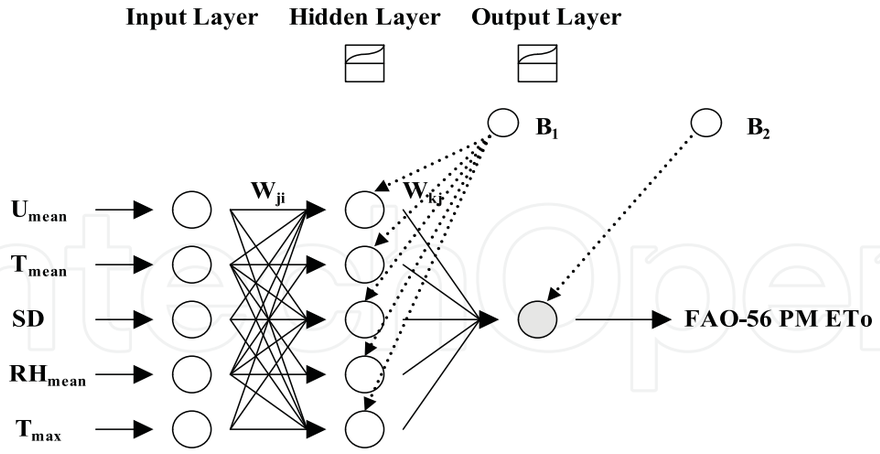


Fig. 2. The developed structure of MLP-NNM with five input nodes

linear discriminant functions. Second, SVM-NNM is motivated by the concept of training and using only those inputs that are near the decision surface since they provide the most information about the classification. The first step in SVM-NNM is transforming the data into a high-dimensional space. This is done using radial basis function (RBF) that places a Gaussian at each sample data. Thus, the feature space becomes as large as the number of sample data. RBF uses backpropagation to train a linear combination of the gaussians to produce the final result. SVM-NNM, however, uses the idea of large margin classifiers for training performance. This decouples the capacity of the classifier from the input space and at the same time provides good generalization. This is an ideal combination for classification (Vapnik, 1992, 2000; Principe et al., 2000; Tripathi et al., 2006).

In this sudy, ε SVM-NNM regression is used. The basic ideas of ε SVM-NNM regression are reviewed. Consider the finite training sample pattern $(x_i, y_i)$, where $x_i \in \Re^n$ is a sample value of the input vector x considering of N training patterns and $y_i \in \Re^n$ is the corresponding value of the desired model output. A nonlinear transformation function $\varphi(\cdot)$ is defined to map the input space to a higher dimension feature space, $\Re^{n_h}$. According to Cover's theorem (Cover, 1965), a linear function, $f(\cdot)$, could be formulated in the high dimensional feature space to look for a nonlinear relationship between inputs and outputs in the original input space. It can be written as equation (3).

$$\bar{y} = f(x) = w^T \varphi(x) + b \tag{3}$$

where $\bar{y}$ = the actual model output. The coefficient w and b are adjustable model parameters. In the ε SVM-NNM regression, we aim at minimizing the emprical risk. It can be written as equation (4).

$$R_{emp} = \frac{1}{N}\sum_{i=1}^{N} \left| y_i - \bar{y}_i \right|_{\varepsilon} \tag{4}$$

where $R_{emp}$ = the empirical risk; and $\left| y_i - \bar{y}_i \right|_{\varepsilon}$ = the Vapnik's ε-insensitive loss function. Following regularization theory (Haykin, 2009), the parameters w and b are estimated by minimizing the cost function. It can be written as equation (5).

$$\psi_{\varepsilon}(w,\xi,\xi^{*}) = \frac{1}{2}w^{T}w + C\sum_{i=1}^{N}(\xi_i + \xi_i^{*}) \tag{5}$$

subject to the constraints ① $y_i - \bar{y}_i \le \varepsilon + \xi_i$ i = 1, 2, ... , N, ② $-y_i + \bar{y}_i \le \varepsilon + \xi_i^{*}$ i = 1, 2, ... , N, and ③ $\xi_i, \xi_i^{*} \ge 0$ i = 1, 2, ... , N. where $\psi_{\varepsilon}(w,\xi,\xi^{*})$ = the cost function; $\xi_i, \xi_i^{*}$ = positive slack variables; and C = the cost constant. The first term of the cost function, which represents weight decay, is used to regularize weight sizes and to penalize large weights. This helps in improving generalization performance (Hush and Horne, 1993). The second term of the cost function, which represents penalty function, penalizes deviations of $\bar{y}$ from y larger than $\pm\varepsilon$ using Vapnik's ε-insensitive loss function. The cost constant C determines the amount up to which deviations from ε are tolerated. Deviations above ε are denoted by $\xi_i$, whereas deviations below – ε are denoted by $\xi_i^{*}$. The constrained quardratic optimization problem can be solved using the method of Lagrangian multipliers (Haykin, 2009). From this solution, the coefficient w can be written as equation (6).

$$w = \sum_{i=1}^{N}(\alpha_i - \alpha_i^{*})\varphi(x_i) \tag{6}$$

where $\alpha_i, \alpha_i^{*}$ = the Lagrange multipliers, which are positive real constants. The data points corresponding to non-zero values for $(\alpha_i - \alpha_i^{*})$ are called support vectors.

In ε SVM-NNM regression to calculate FAO-56 PM ETo, there are several possibilities for the choice of kernel function, including linear, polynomial, sigmoid, splines and RBF. In this study, RBF is used to map the input data into higher dimensional feature space. RBF can be written as the equation (7).

$$k(x,x_j) = \Phi_1 = \exp(-B_1 R_j^2) = \exp\left(-\frac{\left\|x_i - x_j\right\|^2}{2\sigma^2}\right) \tag{7}$$

where i, j = the input layer and the hidden layer; $K(x,x_j) = \Phi_1$ = the inner product kernel function; $B_1 = \frac{1}{2\sigma^2}$, and has a constant value; and σ = the width/spread of RBF, which can be adjusted to control the expressivity of RBF. The function for the single node of the output layer which receives the calculated results of RBF can be written as the equation (8).

$$G_k = [\sum_{j=1}^{N}(\alpha_j - \alpha_j^{*}) \cdot K(x,x_j)] + B \tag{8}$$

where k = the output layer; $G_k$ = the calculated value of the single output node; and B = the bias in the output layer. Finally, equation (8) takes the form of equation (9), which represents ε SVM-NNM regression for modeling of FAO-56 PM ETo.

$$\text{FAO-56 PM ETo} = \Phi_2(G_k) = \Phi_2 \cdot [[\sum_{j=1}^{N}(\alpha_j - \alpha_j^{*}) \cdot K(x,x_j)] + B] \tag{9}$$

where $\Phi_2$ = the linear sigmoid transfer function. A number of SVM-NNM computer programs are now available. DTREG computer program was used to develop SVM-NNM structure. SVM-NNM in the DTREG computer program has been developed and modified using LIBSVM algorithm, a freeware program, developed by Chih-Chung Chang and Chih-Jen Lin (Chang & Lin, 2001). The basic algorithm of LIBSVM is a simplication of both SMO by Platt and SVM Light by Joachims. LIBSVM is capable of C SVM-NNM classification, one-class classification, ν SVM-NNM classification, ν SVM-NNM regression, and ε SVM-NNM regression, respectively. The accuracy of ε SVM-NNM regression is largely dependent on the selection of model parameters such as C, Gamma(γ), and P. DTREG computer program provides two methods, a grid search and a pattern search, for finding optimal parameters values. A grid search tries values of each parameter across the specified search range using geometric steps. A pattern search starts at the center of the search range and makes trial steps in each direction for each parameter. If the fit of model improves, the search center moves to the new point and the process is repeated. If no improvement is found, the step size is reduced and the search is tried again. The pattern search stops when the search step size is reduced to a specified tolerance. Fig. 3 shows the developed structure of SVM-NNM with five input nodes. Table 2 shows the conditions of training performance for SVM-NNM.

| Index | Assigned Value |
|---|---|
| Type of SVM-NNM | ε-SVM regression |
| Kernel Function | RBF |
| Parameter Optimization | Grid search & Pattern search |
| Model Parameters | C, γ, P |
| Training Threshold | 0.001 |

Table 2. Conditions of training performance for SVM-NNM

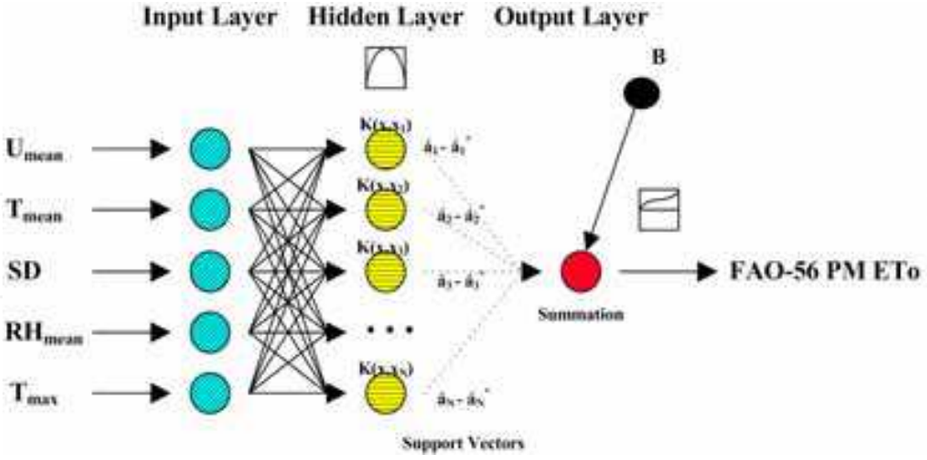


Fig. 3. The developed structure of SVM-NNM with five input nodes

## 4. Study scope and data

The meteorological stations were selected that could represent the entire lands of the Republic of Korea. They were selected from among the 71 meteorological stations including

Jeju-do under the control of the Korea meteorological administration (KMA). The selected meteorological stations should be distributed over the country, and represent each region/county. They should possess long-term climatic data dating back for at least 30 years. Thus, the meteorological stations, which are appropriate for these conditions, include a total of 8 meteorological stations. They are located in Gunsan, Daegu, Seoul, Seongsanpo, Ulsan, Jeonju, Tongyoung, and Haenam. Fig. 4 shows the locations of 8 meteorological stations. The climatic data, which was necessary for MLP-NNM and SVM-NNM application, were collected from the Internet homepage of water management information system (www.wamis.go.kr) and the Korea meteorological administration (www.kma.go.kr). The climatic data available including mean wind speed ($U_{mean}$), mean temperature ($T_{mean}$), sunshine duration (SD), mean relative humidity ($RH_{mean}$), and max temperature ($T_{max}$) were sufficient for MLP-NNM and SVM-NNM application. Furthermore, The climatic data available including maximum temperature ($T_{max}$), minimum temperature ($T_{min}$), mean relative hymidity ($RH_{mean}$), mean wind speed ($U_{mean}$), and sunshine duration (SD) were sufficient for estimating FAO-56 PM ETo using FAO CROPWAT 8.0 computer program. Therefore, the training and testing data were composed using the climatic data in daily units from 01/01/1985 to 12/31/1992.


Fig. 4. The locations of 8 meteorological stations, Republic of Korea

## 5. Application of MLP-NNM and SVM-NNM

### 5.1 Performance statistics

The performance of MLP-NNM and SVM-NNM to account for calculating the daily FAO-56 PM ETo was evaluated using a wide variety of standard statistics index. A total of three different standard statistics index were employed; the coefficient of correlation (CC), root mean square error (RMSE), and Nash-Sutcliffe coefficient ($R^2$) (Nash & Sutcliffe, 1970; ASCE, 1993). Table 3 shows summary of the statistics index in this study. where $\overline{y_i}(x)$ = the calculated FAO-56 PM ETo (mm/day); $y_i(x)$ = the observed FAO-56 PM ETo (mm/day); $\overline{u_i}$ = mean of the calculated FAO-56 PM ETo (mm/day); $u_y$ = mean of the observed FAO-56

PM ETo (mm/day); and n = total number of the daily FAO-56 PM ETo considered. A model which is effective in the modeling of FAO-56 PM ETo accurately, and efficient in capturing the complex relationship among the various inputs and output variables involved in a particular problem, is considered the best. CC, RMSE, and $R^2$ statistics quantify the efficiency of MLP-NNM and SVM-NNM in capturing the extremely complex, dynamic, nonlinear, and fragmented rainfall-runoff relationships (Kim et al., 2009).

### 5.2 Input nodes determination

At the beggining of this study, the input nodes of MLP-NNM and SVM-NNM had to be determined. From the previous literatures on the ET modeling using the neural networks models, five kinds of climatic data available, which were used to cite frequently were determined. The climatic data available were mean wind speed ($U_{mean}$), mean temperature ($T_{mean}$), sunshine duration (SD), mean relative humidity ($RH_{mean}$), and max temperature ($T_{max}$). Therefore, MLP-NNM and SVM-NNM was prior fed with the mean wind speed ($U_{mean}$), which was the most frequently cited by the previous researchers. It was adopted as the minimum input combinations represented by MLP 1 and SVM 1 for determining the optimal input combinations. Then, the best network configuration determined was used to train and test the several other input combinations. MLP 2 and SVM 2 have two input nodes; mean wind speed ($U_{mean}$) and mean temperature ($T_{mean}$). MLP 3 and SVM 3 have three input nodes; mean wind speed ($U_{mean}$), mean temperature ($T_{mean}$), and sunshine duration (SD). MLP 4 and SVM 4 have four input nodes; mean wind speed ($U_{mean}$), mean temperature ($T_{mean}$), sunshine duration (SD), and mean relative humidity ($RH_{mean}$). Finally, MLP 5 and SVM 5 have five input nodes; mean wind speed ($U_{mean}$), mean temperature ($T_{mean}$), sunshine duration (SD), mean relative humidity ($RH_{mean}$), and max temperature ($T_{max}$). Table 4 shows the input combinations of MLP-NNM and SVM-NNM.

| Statistics Index | Equation |
|---|---|
| CC | $\frac{\frac{1}{n}\sum_{i=1}^{n}[y_i(x)-u_y][\bar{y}_i(x)-\bar{u}_y]}{\sqrt{\frac{1}{n}\sum_{i=1}^{n}[y_i(x)-u_y]^2}\sqrt{\frac{1}{n}\sum_{i=1}^{n}[\bar{y}_i(x)-\bar{u}_y]^2}}$ |
| RMSE | $\sqrt{\frac{1}{n}\sum_{i=1}^{n}[\bar{y}_i(x)-y_i(x)]^2}$ |
| $R^2$ | $1-\frac{\sum_{i=1}^{n}[y_i(x)-\bar{y}_i(x)]^2}{\sum_{i=1}^{n}[y_i(x)-u_y]^2}$ |

Table 3. Summary of statistics index

| Neural Networks Model | | Input Combinations |
|---|---|---|
| MLP-NNM | SVM-NNM | |
| MLP 1 | SVM 1 | $U_{mean}$ |
| MLP 2 | SVM 2 | $U_{mean}$, $T_{mean}$ |
| MLP 3 | SVM 3 | $U_{mean}$, $T_{mean}$, SD, |
| MLP 4 | SVM 4 | $U_{mean}$, $T_{mean}$, SD, $RH_{mean}$ |
| MLP 5 | SVM 5 | $U_{mean}$, $T_{mean}$, SD, $RH_{mean}$ , $T_{max}$ |

Table 4. Input combinations of MLP-NNM and SVM-NNM

### 5.3 Data normalization

The data used in this study including mean wind speed ($U_{mean}$), mean temperature ($T_{mean}$), sunshine duration (SD), mean relative humidity ($RH_{mean}$), and max temperature ($T_{max}$) were nomalized for preventing and overcomining problem associated with the extreme values. An important reason for the normalization of input nodes is that each of input nodes represents an observed value in a different unit. Such input nodes are normalized, and the input nodes in non-dimension unit are relocated. The similarity effect of input nodes is thus eliminated (Kim et al., 2009). According to Zanetti et al. (2007), by grouping the daily values into averages, ETo may be estimated due to their highest stabilization. For data normalization, the data of input and output nodes were scaled in the range of [0 1] using the equation (10).

$$Y_{norm} = \frac{Y_i - Y_{min}}{Y_{max} - Y_{min}} \tag{10}$$

where $Y_{norm}$ = the normalized dimensionless data of the specific input node; $Y_i$ = the observed data of the specific input node; $Y_{min}$ = the minimum data of the specific input node; and $Y_{max}$ = the maximum data of the specific input node.

### 5.4 Training performance

The method for estimating parameters is generally called the training performance in the neural networks model category. The training performance of neural networks model is iterated until the training error is reached to the training tolerance. Iteration means one completely pass through a set of inputs and target patterns or data. In general, it is assumed that the neural networks model does not have any prior knowledge about the example problem before it is trained. A difficult task with the neural networks model is to choose the number of hidden nodes. The network geometry is problem dependent. This study adopted one hidden layer for the construction of MLP-NNM and SVM-NNM since it is well known that one hidden layer is enough to represent the ETo nonlinear complex relationship (Kumar et al., 2002; Zanetti et al., 2007). The number of hidden nodes was determined as five for MLP-NNM with the various input combinations (MLP 1, MLP 2, MLP 3, MLP 4, and MLP 5). In SVM-NNM, however, the number of hidden nodes was determined by the training performance of SVM-NNM with the various input combinations (SVM 1, SVM 2, SVM 3, SVM 4, and SVM 5). Kisi (2007) varied the hidden nodes between 2 and 6 after trial and error method for Claremont, Ponoma, and Santa Monica stations, respectively. For three stations, the optimal number of hidden nodes was found at six based on minimum mean

square error (MSE), minimum mean absolute error (MAE), and maximum determination coefficient ($R^2$). Khoob (2008a, b) trained the neural networks models with up to thirty hidden nodes using similar inputs set and found optimal results at six and nine hidden nodes in Safiabad and Khuzestan plain, respectively. For the training data of MLP-NNM and SVM-NNM, the six-year data from 01/01/1985 to 12/31/1990 in 8 meteorological stations were used. The total amount of data used for the training performance was composed of 2191 data for daily time series.

### 5.4.1 Results of MLP-NNM training performance

For the training performance of MLP-NNM, NeuroSolutions 5.0 computer program was used to carry out the training performance. Fig. 5 shows the building processes of MLP-NNM training performance using NueroSolution 5.0 computer program. Table 5 shows the summary of optimal MLP-NNM statistics results during the training performance for 8 meteorological stations. For 8 meteorological stations, the best statistics results were found at MLP 4 and MLP 5 on average. In Gunsan station, the performance statistics results of MLP 5 were 0.968, 0.365 (mm/day), and 0.936 for CC, RMSE, and $R^2$, respectively. In Daegu station, the performance statistics results of MLP 5 were 0.975, 0.364 (mm/day), and 0.950 for CC, RMSE, and $R^2$, respectively. In Seoul station, the performance statistics results of MLP 4 were 0.963, 0.413 (mm/day), and 0.927 for CC, RMSE, and $R^2$, respectively. In Seonsganpo station, the performance statistics results of MLP 4 were 0.842, 0.676 (mm/day), and 0.710 for CC, RMSE, and $R^2$, respectively. In Ulsan station, the performance statistics results of MLP 4 were 0.956, 0.412 (mm/day), and 0.914 for CC, RMSE, and $R^2$, respectively. In Jeonju station, the performance statistics results of MLP 5 were 0.966, 0.383 (mm/day), and 0.932 for CC, RMSE, and $R^2$, respectively. In Tongyoung station, the performance statistics results of MLP 5 were 0.945, 0.438 (mm/day), and 0.893 for CC, RMSE, and $R^2$, respectively. In Haenam station, the performance statistics results of MLP 4 were 0.959, 0.396 (mm/day), and 0.919 for CC, RMSE, and $R^2$, respectively. From the evaluation of MLP-NNM training performance, MLP 4 and MLP5 was found to show the better statistics results compared with MLP 1, MLP 2, and MLP 3.

| Station | Model | CC | RMSE (mm/day) | $R^2$ |
|---|---|---|---|---|
| Gunsan | MLP 5 | 0.968 | 0.365 | 0.936 |
| Daegu | MLP 5 | 0.975 | 0.364 | 0.950 |
| Seoul | MLP 4 | 0.963 | 0.413 | 0.927 |
| Seongsanpo | MLP 4 | 0.842 | 0.676 | 0.710 |
| Ulsan | MLP 4 | 0.956 | 0.412 | 0.914 |
| Jeonju | MLP 5 | 0.966 | 0.383 | 0.932 |
| Tongyoung | MLP 5 | 0.945 | 0.438 | 0.893 |
| Haenam | MLP 4 | 0.959 | 0.396 | 0.919 |

Table 5. Summary of optimal MLP-NNM statistics results during the training performance

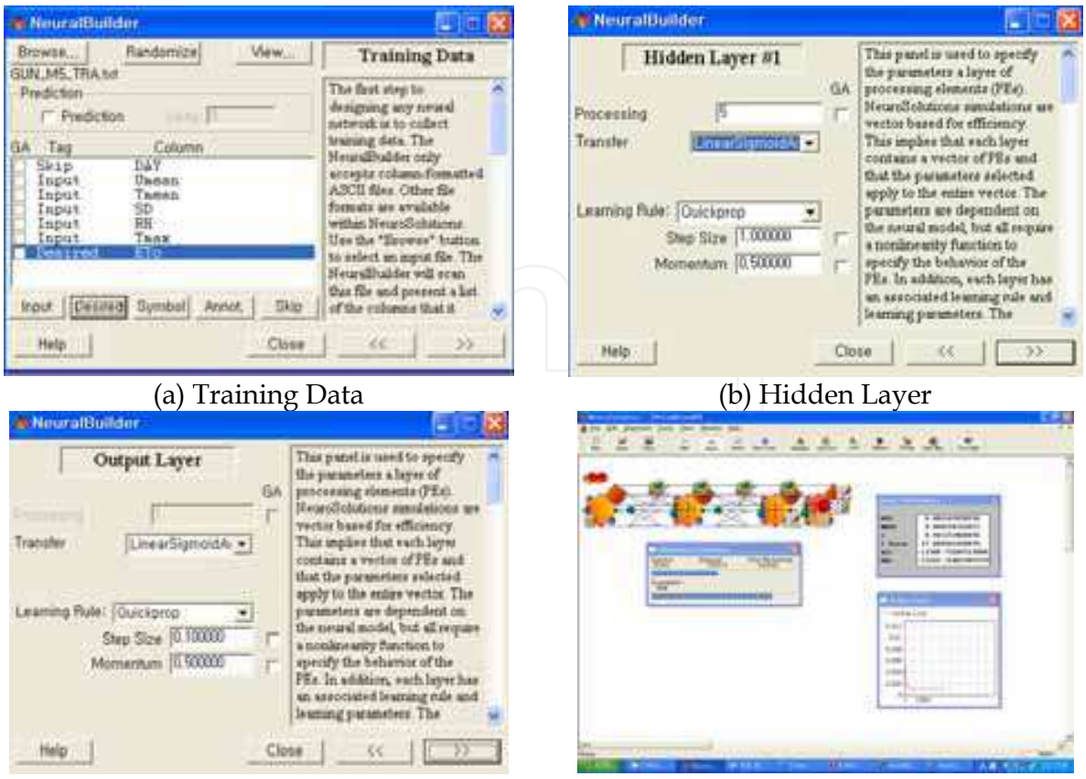


(a) Training Data (b) Hidden Layer

(c) Output Layer (d) Training Performance

Fig. 5. The building precesses of MLP-NNM training performance using NueroSolution 5.0

### 5.4.2 Results of SVM-NNM training performance

For the training performance of SVM-NNM, DTREG computer program was used to carry out the training performance. Fig. 6 shows the building processes of SVM-NNM training performance using DTREG computer program. Table 6 shows the summary of optimal SVM-NNM statistics results during the training performance for 8 meteorological stations.

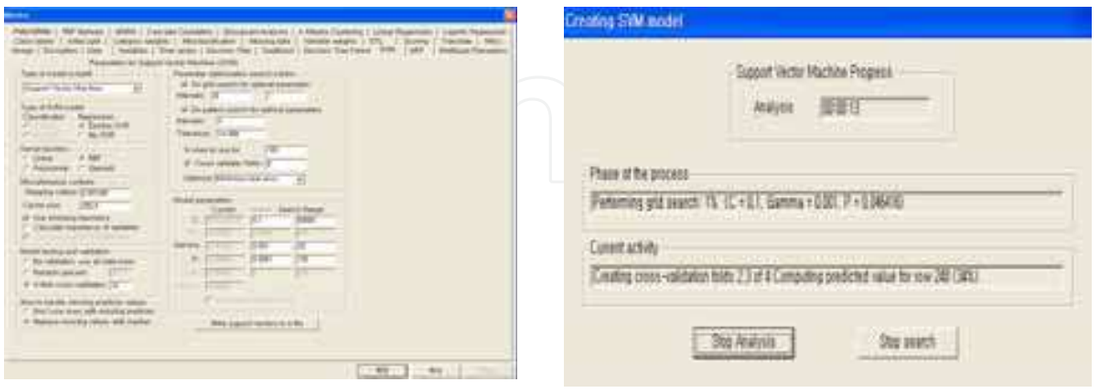


(a) Training Category (b) Training Performance

Fig. 6. The building precesses of SVM-NNM training performance using DTREG

For 8 meteorological stations, the best statistics results were found at SVM 5. In Gunsan station, the performance statistics results of SVM 5 were 0.982, 0.274 (mm/day), and 0.964

for CC, RMSE, and $R^2$, respectively. In Daegu station, the performance statistics results of SVM 5 were 0.985, 0.278 (mm/day), and 0.971 for CC, RMSE, and $R^2$, respectively. In Seoul station, the performance statistics results of SVM 5 were 0.979, 0.315 (mm/day), and 0.957 for CC, RMSE, and $R^2$, respectively. In Seonsganpo station, the performance statistics results of SVM 5 were 0.857, 0.670 (mm/day), and 0.715 for CC, RMSE, and $R^2$, respectively. In Ulsan station, the performance statistics results of SVM 5 were 0.970, 0.336 (mm/day), and 0.940 for CC, RMSE, and $R^2$, respectively. In Jeonju station, the performance statistics results of SVM 5 were 0.979, 0.304 (mm/day), and 0.957 for CC, RMSE, and $R^2$, respectively. In Tongyoung station, the performance statistics results of SVM 5 were 0.963, 0.362 (mm/day), and 0.927 for CC, RMSE, and $R^2$, respectively. In Haenam station, the performance statistics results of SVM 5 were 0.971, 0.334 (mm/day), and 0.943 for CC, RMSE, and $R^2$, respectively. From the evaluation of SVM-NNM training performance, SVM 5 was found to show the better statistics results compared with SVM 1, SVM 2, SVM 3 and SVM 4. Furthermore, from the statistics results of training peformance for MLP-NNM and SVM-NNM, we could conclude that the statistics results of SVM-NNM were better than those of MLP-NNM.

| Station | Model | CC | RMSE (mm/day) | $R^2$ |
|---|---|---|---|---|
| Gunsan | SVM 5 | 0.982 | 0.274 | 0.964 |
| Daegu | SVM 5 | 0.985 | 0.278 | 0.971 |
| Seoul | SVM 5 | 0.979 | 0.315 | 0.957 |
| Seongsanpo | SVM 5 | 0.857 | 0.670 | 0.715 |
| Ulsan | SVM 5 | 0.970 | 0.336 | 0.940 |
| Jeonju | SVM 5 | 0.979 | 0.304 | 0.957 |
| Tongyoung | SVM 5 | 0.963 | 0.362 | 0.927 |
| Haenam | SVM 5 | 0.971 | 0.334 | 0.943 |

Table 6. Summary of optimal SVM-NNM statistics results during training performance

### 5.5 Testing performance

Neural networks model is tested by determining whether the model meets the objectives of modeling within some preestablished criteria or not. Of course, the optimal parameters, which are determined during the training performance, are applied in the testing performance of neural networks model (Kim, 2004). For the testing data of MLP-NNM and SVM-NNM, the two-year data from 01/01/1991 to 12/31/1992 in 8 meteorological stations were used. The total amount of data used for the testing performance was composed of 731 data for daily time series. Generally, a maximum of 40% of the total training data are used as the testing data. The testing performance applied the cross-validation method in order to overcome the over-fitting problem of MLP-NNM and SVM-NNM. The cross-validation method is not to train all the training data until MLP-NNM and SVM-NNM reaches the minimum RMSE, but is to cross-validate with the testing data at the end of each training performance. If the over-fitting problem occurs, the convergence process over the mean square error of the testing data will not decrease but will increase as the training data are still trained (Bishop, 1994; Haykin, 2009). Furthermore, the statistics results of testing performance for MLP-NNM and SVM-NNM were compared with those of multiple linear regression model (MLRM).

### 5.5.1 Results of MLP-NNM testing performance

For the testing performance of MLP-NNM, NeuroSolutions 5.0 computer program was used to carry out the testing performance based on the statistics results of training performance. For 8 meteorological stations, the best statistics results were found at MLP 4 and MLP 5 on average. In Gunsan station, the performance statistics results of MLP 5 were 0.964, 0.369 (mm/day), and 0.928 for CC, RMSE, and $R^2$, respectively. In Daegu station, the performance statistics results of MLP 5 were 0.980, 0.349 (mm/day), and 0.961 for CC, RMSE, and $R^2$, respectively. In Seoul station, the performance statistics results of MLP 4 were 0.966, 0.402 (mm/day), and 0.933 for CC, RMSE, and $R^2$, respectively. In Seonsganpo station, the performance statistics results of MLP 4 were 0.955, 0.481 (mm/day), and 0.867 for CC, RMSE, and $R^2$, respectively. In Ulsan station, the performance statistics results of MLP 4 were 0.958, 0.398 (mm/day), and 0.918 for CC, RMSE, and $R^2$, respectively. In Jeonju station, the performance statistics results of MLP 5 were 0.959, 0.411 (mm/day), and 0.918 for CC, RMSE, and $R^2$, respectively. In Tongyoung station, the performance statistics results of MLP 5 were 0.949, 0.435 (mm/day), and 0.896 for CC, RMSE, and $R^2$, respectively. In Haenam station, the performance statistics results of MLP 4 were 0.956, 0.410 (mm/day), and 0.914 for CC, RMSE, and $R^2$, respectively. From the evaluation of MLP-NNM testing performance, MLP 4 and MLP5 was found to show the better statistics results compared with MLP 1, MLP 2, and MLP 3. The statistics results of testing performance were similar with those of training performance for MLP-NNM. In Gunsan, Jeonju, Haenam stations, the statistics results of training performance were better than those of testing performance. In Daegu, Seoul, Seongsanpo, Ulsan, and Tongyoung stations, vice versa. Table 7 shows the summary of optimal MLP-NNM statistics results during the testing performance for 8 meteorological stations. And, MLP 1 using only mean wind speed ($U_{mean}$) performed the worst results. However, adding mean temperature ($T_{mean}$) into the input combinations significantly increased the statistics results of testing performance. We can consider that adding the climatic variables into the input combinations increases the statistics results of testing performance for MLP-NNM. It can obviously be seen from CC, RMSE, and $R^2$ statistics of MLP-NNM. Table 8 shows the statistics results of each MLP-NNM for Daegu, Ulsan, Jeonju, and Tongyoung stations during the testing performance. Fig. 7 shows the comparison plots of observed and calculated FAO-56 PM ETo for optimal MLP-NNM. Fig. 8 shows the scatter plots between FAO-56 PM ETo and optimal MLP-NNM ETo.

| Station | Model | CC | RMSE (mm/day) | $R^2$ |
|---|---|---|---|---|
| Gunsan | MLP 5 | 0.964 | 0.369 | 0.928 |
| Daegu | MLP 5 | 0.980 | 0.349 | 0.961 |
| Seoul | MLP 4 | 0.966 | 0.402 | 0.933 |
| Seongsanpo | MLP 4 | 0.955 | 0.481 | 0.867 |
| Ulsan | MLP 4 | 0.958 | 0.398 | 0.918 |
| Jeonju | MLP 5 | 0.959 | 0.411 | 0.918 |
| Tongyoung | MLP 5 | 0.949 | 0.435 | 0.896 |
| Haenam | MLP 4 | 0.956 | 0.410 | 0.914 |

Table 7. Summary of optimal MLP-NNM statistics results during the testing performance

| Station | Statistics Index | Model Category | | | | |
|---|---|---|---|---|---|---|
| | | MLP 1 | MLP 2 | MLP 3 | MLP 4 | MLP 5 |
| Daegu | CC | 0.389 | 0.808 | 0.950 | 0.978 | 0.980 |
| | RMSE (mm/day) | 1.653 | 1.056 | 0.560 | 0.369 | 0.349 |
| | $R^2$ | 0.129 | 0.644 | 0.900 | 0.957 | 0.961 |
| Ulsan | CC | 0.341 | 0.748 | 0.931 | 0.958 | 0.942 |
| | RMSE (mm/day) | 1.325 | 0.920 | 0.509 | 0.398 | 0.471 |
| | $R^2$ | 0.086 | 0.559 | 0.865 | 0.918 | 0.884 |
| Jeonju | CC | 0.293 | 0.802 | 0.947 | 0.950 | 0.959 |
| | RMSE (mm/day) | 1.375 | 0.858 | 0.460 | 0.448 | 0.411 |
| | $R^2$ | 0.077 | 0.641 | 0.897 | 0.902 | 0.918 |
| Tongyoung | CC | 0.368 | 0.739 | 0.933 | 0.932 | 0.949 |
| | RMSE (mm/day) | 1.288 | 0.913 | 0.534 | 0.497 | 0.435 |
| | $R^2$ | 0.091 | 0.544 | 0.844 | 0.865 | 0.897 |

Table 8. Statistics results of each MLP-NNM during the testing performance

#### 5.5.2 Results of SVM-NNM testing performance

For the testing performance of SVM-NNM, DTREG computer program was used to carry out the testing performance based on the statistics results of the training performance. For 8 meteorological stations, the best statistics results were found at SVM 5. In Gunsan station, the performance statistics results of SVM 5 were 0.983, 0.255 (mm/day), and 0.965 for CC, RMSE, and $R^2$, respectively. In Daegu station, the performance statistics results of SVM 5 were 0.990, 0.255 (mm/day), and 0.979 for CC, RMSE, and $R^2$, respectively. In Seoul station, the performance statistics results of SVM 5 were 0.985, 0.267 (mm/day), and 0.971 for CC, RMSE, and $R^2$, respectively. In Seonsganpo station, the performance statistics results of SVM 5 were 0.970, 0.332 (mm/day), and 0.937 for CC, RMSE, and $R^2$, respectively. In Ulsan station, the performance statistics results of SVM 5 were 0.971, 0.329 (mm/day), and 0.944 for CC, RMSE, and $R^2$, respectively. In Jeonju station, the performance statistics results of SVM 5 were 0.976, 0.311 (mm/day), and 0.953 for CC, RMSE, and $R^2$, respectively. In Tongyoung station, the performance statistics results of SVM 5 were 0.968, 0.353 (mm/day), and 0.932 for CC, RMSE, and $R^2$, respectively. In Haenam station, the performance statistics results of SVM 5 were 0.976, 0.307 (mm/day), and 0.951 for CC, RMSE, and $R^2$, respectively. From the evaluation of SVM-NNM testing performance, SVM 5 was found to show the better statistics results compared with SVM 1, SVM 2, SVM 3, and SVM 4. The statistics results of testing performance were similar with those of training performance for SVM-NNM. In every station except for Jeonju station, the statistics results of testing performance were better than those of training performance. In Jeonju station, vice versa. Table 9 shows the summary of optimal SVM-NNM statistics results during the testing performance for 8 meteorological stations. And, SVM 1 using only mean wind speed ($U_{mean}$) performed the worst results. However, adding mean temperature ($T_{mean}$) into the input combinations significantly increased the statistics results of testing performance. We can consider that adding the climatic variables into the input combinations increases the statistics results of testing performance for SVM-NNM. It can obviously be seen from CC, RMSE, and $R^2$ statistics of SVM-NNM. Table 10 shows the statistics results of each SVM-NNM for Daegu, Ulsan, Jeonju, and Tongyoung stations during the testing performance. Fig. 9 shows

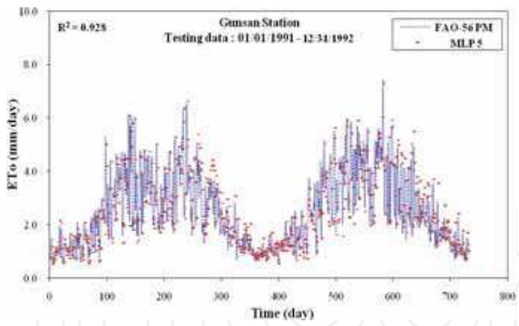


(a) Gunsan

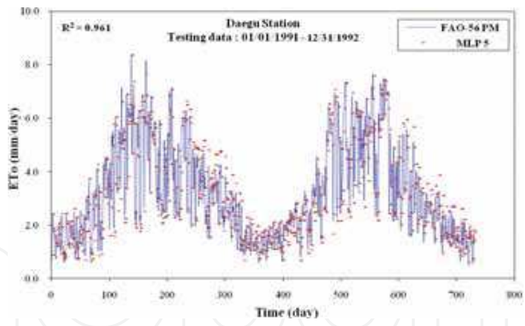


(b) Daegu

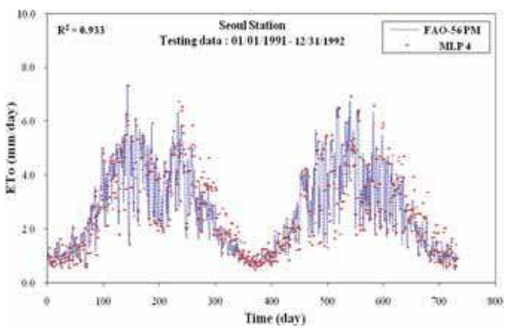


(c) Seoul

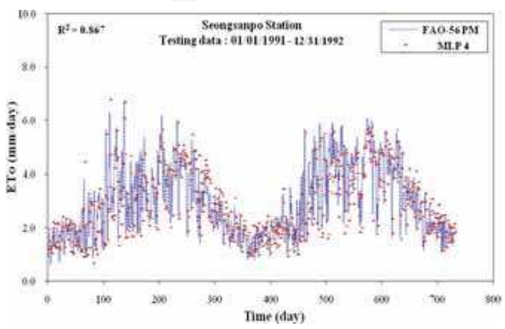


(d) Seongsanpo

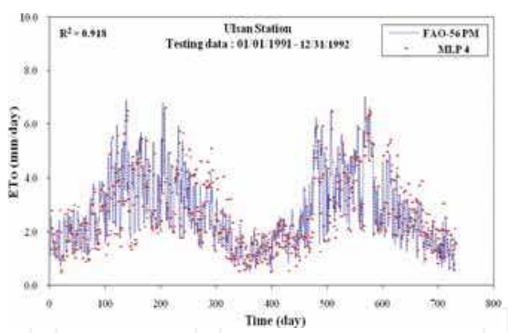


(e) Ulsan

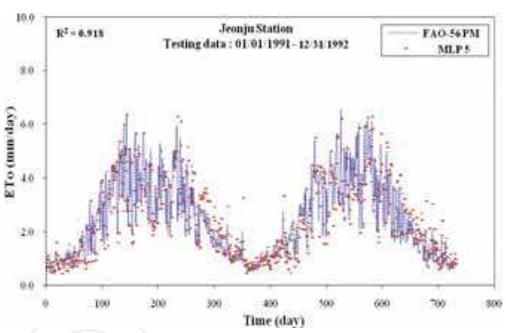


(f) Jeonju

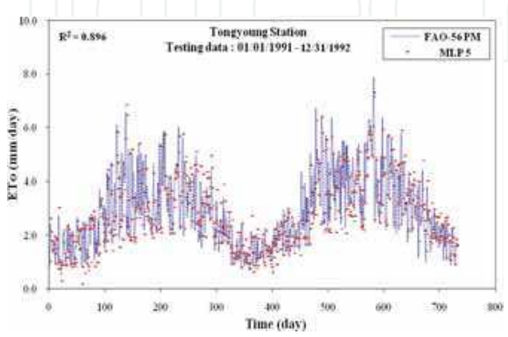


(g) Tongyoung

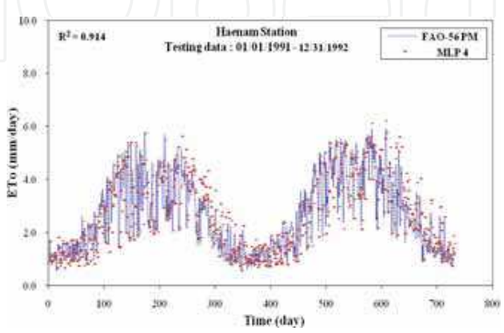


(h) Haenam

Fig. 7. Comparison plots of observed and calculated FAO-56 PM ETo

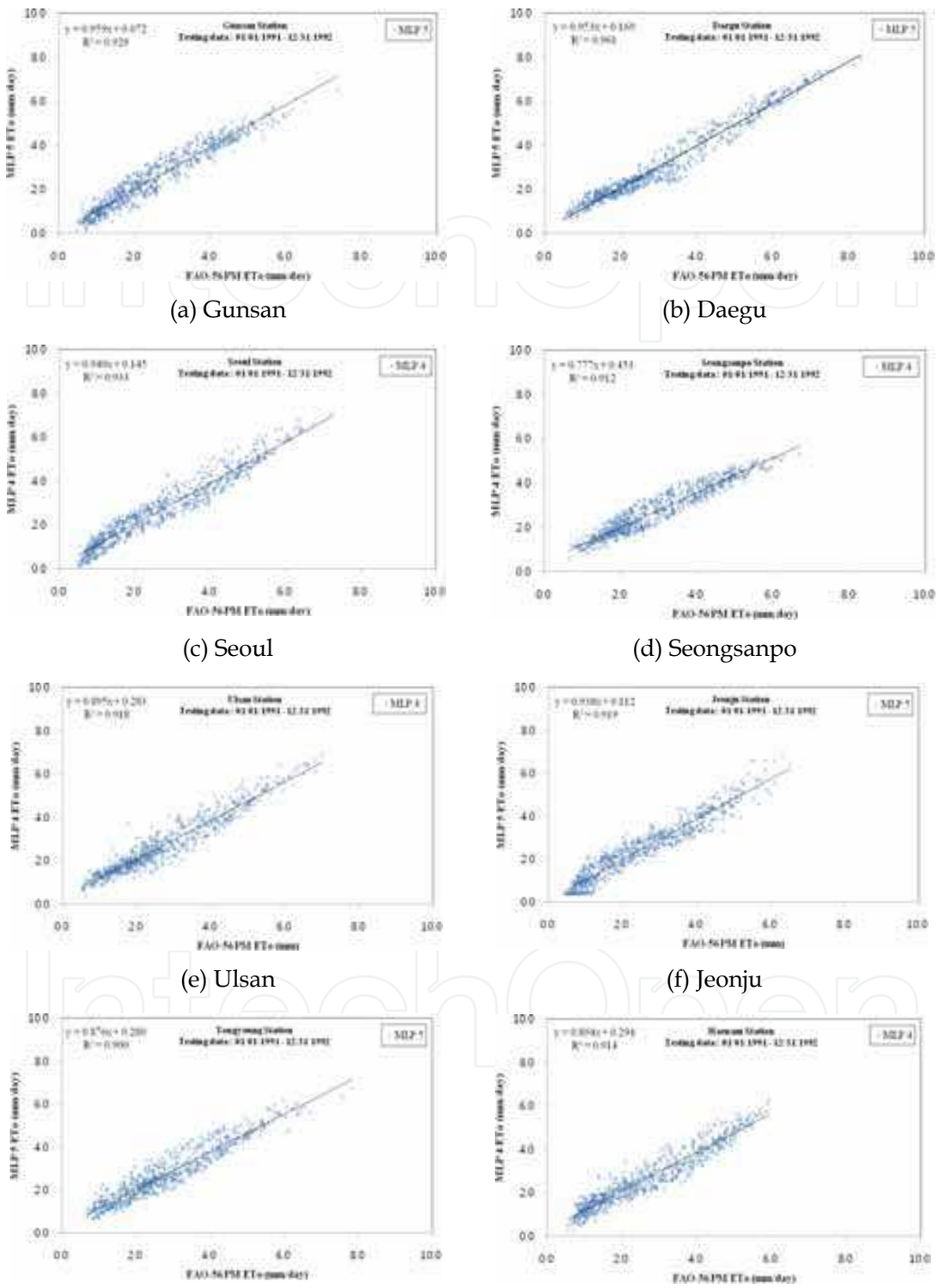

(a) Gunsan (b) Daegu

(c) Seoul (d) Seongsanpo

(e) Ulsan (f) Jeonju

(g) Tongyoung (h) Haenam

Fig. 8. Scatter plots between FAO-56 PM ETo and optimal MLP-NNM ETo

the comparisons of observed and calculated FAO-56 PM ETo for the testing performance of optimal SVM-NNM. Fig. 10 shows the scatter plots between FAO-56 PM ETo and optimal SVM-NNM ETo. From the comparison of testing performance for MLP-NNM and SVM-NNM, the statistics results of SVM-NNM were better than those of MLP-NNM based on CC, RMSE, and $R^2$ statistics. We can consider that the performance of SVM-NNM is better than that of MLP-NNM for the modeling of nonlinear time series such as the FAO-56 PM ETo, which includes the natural uncertainty.

| Station | Model | CC | RMSE (mm/day) | $R^2$ |
|---|---|---|---|---|
| Gunsan | SVM 5 | 0.983 | 0.255 | 0.965 |
| Daegu | SVM 5 | 0.990 | 0.255 | 0.979 |
| Seoul | SVM 5 | 0.985 | 0.267 | 0.971 |
| Seongsanpo | SVM 5 | 0.970 | 0.332 | 0.937 |
| Ulsan | SVM 5 | 0.971 | 0.329 | 0.944 |
| Jeonju | SVM 5 | 0.976 | 0.311 | 0.953 |
| Tongyoung | SVM 5 | 0.968 | 0.351 | 0.932 |
| Haenam | SVM 5 | 0.976 | 0.307 | 0.951 |

Table 9. Summary of optimal SVM-NNM statistical results during the testing performance

| Station | Statistics Index | Model Category | | | | |
|---|---|---|---|---|---|---|
| | | SVM 1 | SVM 2 | SVM 3 | SVM 4 | SVM 5 |
| Daegu | CC | 0.345 | 0.829 | 0.963 | 0.984 | 0.990 |
| | RMSE (mm/day) | 1.706 | 1.004 | 0.484 | 0.313 | 0.255 |
| | $R^2$ | 0.072 | 0.679 | 0.925 | 0.969 | 0.979 |
| Ulsan | CC | 0.363 | 0.767 | 0.953 | 0.970 | 0.971 |
| | RMSE (mm/day) | 1.318 | 0.894 | 0.424 | 0.336 | 0.329 |
| | $R^2$ | 0.096 | 0.584 | 0.906 | 0.941 | 0.944 |
| Jeonju | CC | 0.332 | 0.823 | 0.962 | 0.966 | 0.976 |
| | RMSE (mm/day) | 1.394 | 0.828 | 0.399 | 0.372 | 0.311 |
| | $R^2$ | 0.052 | 0.665 | 0.922 | 0.933 | 0.953 |
| Tongyoung | CC | 0.378 | 0.781 | 0.946 | 0.966 | 0.968 |
| | RMSE (mm/day) | 1.321 | 0.856 | 0.473 | 0.352 | 0.351 |
| | $R^2$ | 0.044 | 0.599 | 0.877 | 0.932 | 0.932 |

Table 10. Statistics results of each SVM-NNM during the testing performance

#### 5.5.3 Application and comparison of Multiple Linear Regression Model (MLRM)

The potential of MLP-NNM and SVM-NNM was tested for the application and comparison of multiple linear regression model (MLRM). The statistics result of testing performance for MLP-NNM and SVM-NNM were compared with those of MLRM. MLRM is important because the model enables more than one independent variable to be included in the structure. This can lead to significant increases in calculation accuracy and the ability to measure the effect of each X variable on Y. MLRM should provide more stable estimates of Y since calculations with the bivariate equation are subject to fluctuations due to extreme

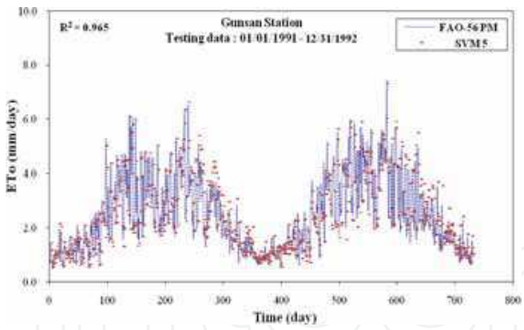


(a) Gunsan

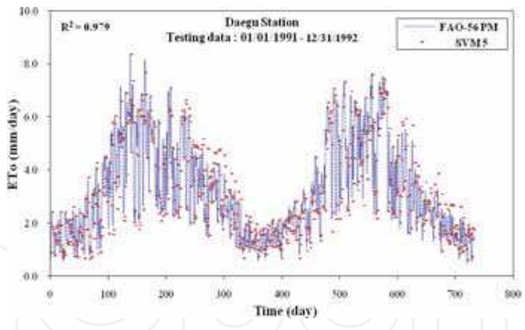


(b) Daegu

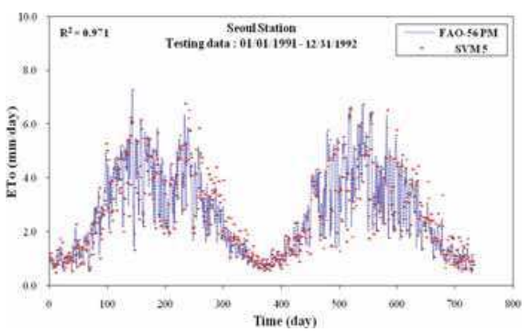


(c) Seoul

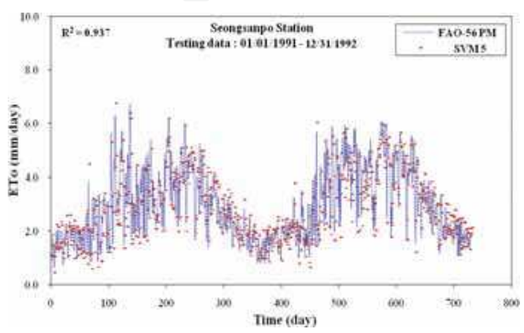


(d) Seongsanpo

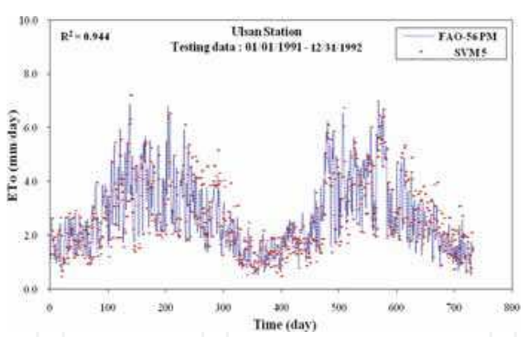


(e) Ulsan

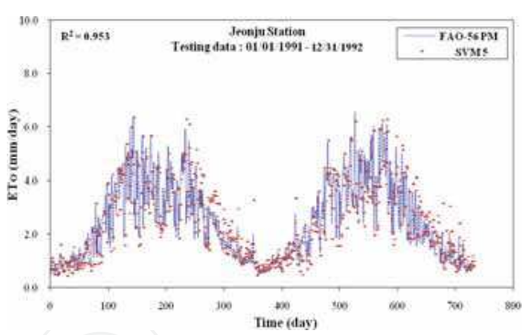


(f) Jeonju

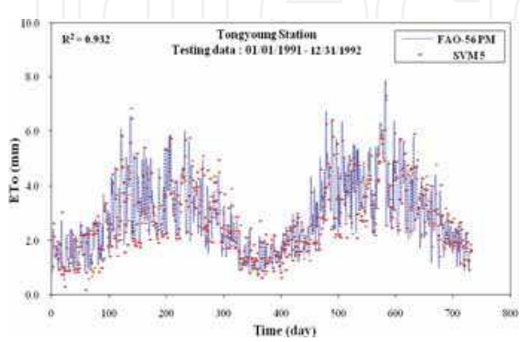


(g) Tongyoung

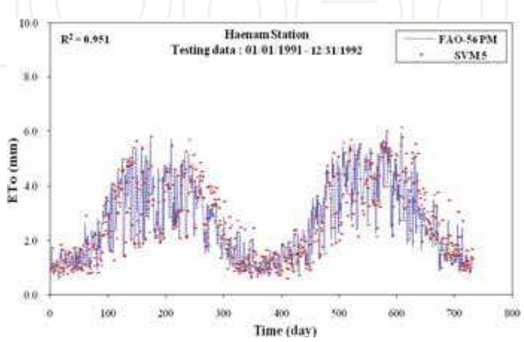


(h) Haenam

Fig. 9. Comparison plots of observed and calculated FAO-56 PM ETo

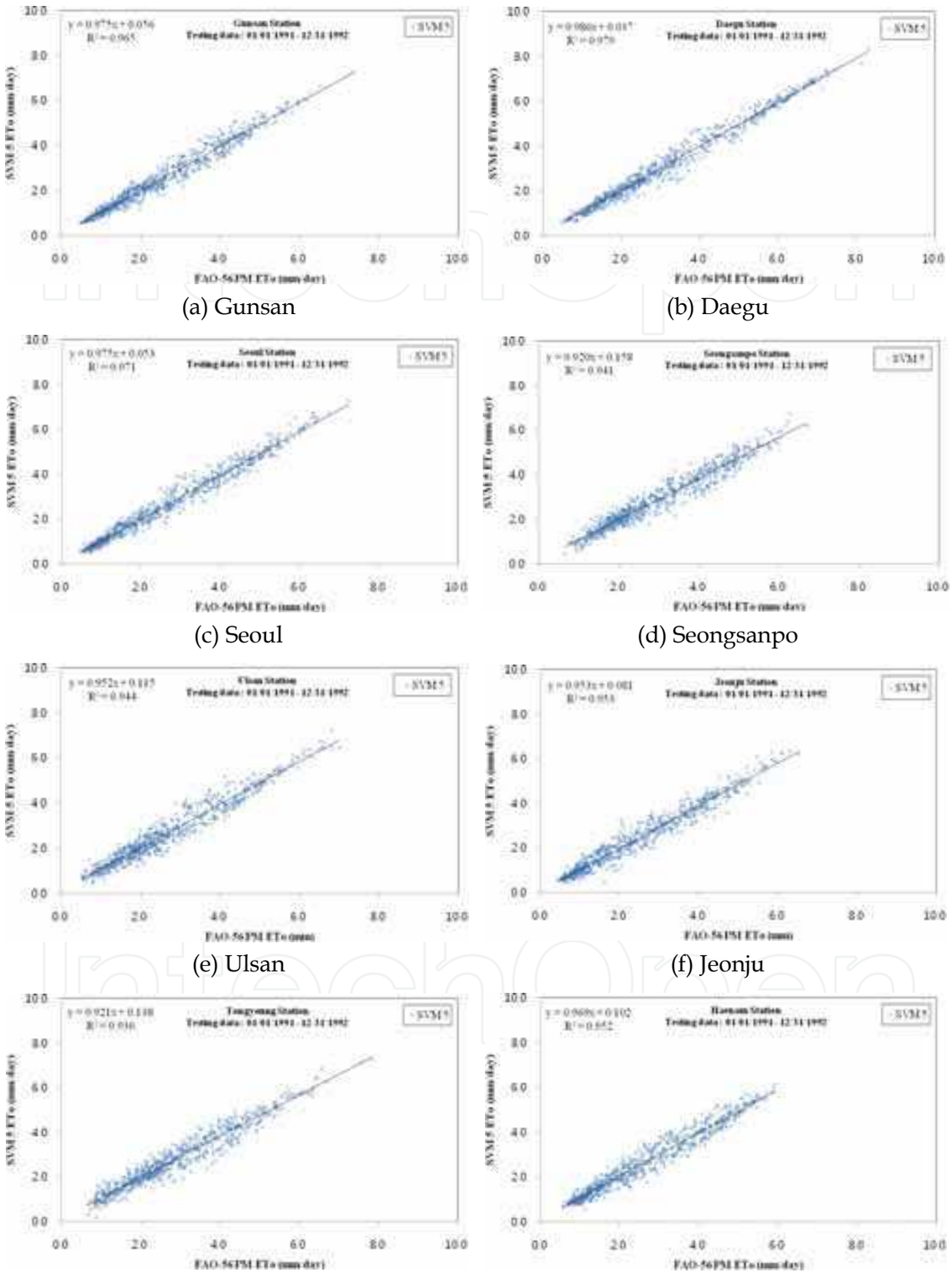

(a) Gunsan (b) Daegu

(c) Seoul (d) Seongsanpo

(e) Ulsan (f) Jeonju

(g) Tongyoung (h) Haenam

Fig. 10. Scatter plots between FAO-56 PM ETo and optimal SVM-NNM ETo

variations in X. When the model includes more than one independent variable, extreme variation in one independent variable is less likely to cause extreme variation in the calculated values of Y (McCuen, 1993; Kottegoda, 1998; Salas et al., 2005). From the statistics results of testing performance for MLP-NNM and SVM-NNM, the best statistics results were found at MLP 4 and MLP 5 on average for MLP-NNM. The best statistics results, furthermore, were found at SVM 5 for SVM-NNM. So, two types of MLRM are adopted; MLRM 1 and MLRM 2. MLRM 1 has four independent variables including mean wind speed ($U_{mean}$), mean temperature ($T_{mean}$), sunshine duration (SD), and mean relative humidity ($RH_{mean}$). And, MLRM 2 has five independent variables including mean wind speed ($U_{mean}$), mean temperature ($T_{mean}$), sunshine duration (SD), mean relative humidity ($RH_{mean}$), and max temperature ($T_{max}$). That is, MLRM 1 corresponds to MLP 4 and SVM 4, and MLRM 2 corresponds to MLP 5 and SVM 5. MLRM 1 and MLRM 2 can be written as the equation (11) and (12).

$$\text{FAO-56 PM ETo} = b_0 + b_1 U_{mean} + b_2 T_{mean} + b_3 SD + b_4 RH_{mean} \tag{11}$$

$$\text{FAO-56 PM ETo} = b_0 + b_1 U_{mean} + b_2 T_{mean} + b_3 SD + b_4 RH_{mean} + b_5 T_{max} \tag{12}$$

where $b_i (i = 1,2,\ldots,p) =$ the slope coefficient, which is also known as the regression coefficient because it is claculated by the results of regression analysis, and $b_0$ = intercept. In this study, the slope coefficients of MLRM 1 and MLRM 2 were calculated using the training data, which were used for MLP-NNM and SVM-NNM. Table 11 shows equations of MLRM 1 and MLRM 2 calculated by the training data for Daegu, Ulsan, Jeonju, and Tongyoung stations, respectively.

| Station | Model Type | Equation |
|---|---|---|
| Daegu | MLRM 1 | FAO-56 PM ETo = 2.894+0.125$U_{mean}$+0.148$T_{mean}$+0.135SD-0.044$RH_{mean}$ |
| | MLRM 2 | FAO-56 PM ETo = 2.099+0.192$U_{mean}$+0.041$T_{mean}$+0.100SD-0.041$RH_{mean}$+0.108$T_{max}$ |
| Ulsan | MLRM 1 | FAO-56 PM ETo = 0.834+0.204$U_{mean}$+0.136$T_{mean}$+0.169SD-0.020$RH_{mean}$ |
| | MLRM 2 | FAO-56 PM ETo =0.552+0.237$U_{mean}$+0.094$T_{mean}$+0.156SD-0.019$RH_{mean}$+0.044 $T_{max}$ |
| Jeonju | MLRM 1 | FAO-56 PM ETo = 1.743+0.294$U_{mean}$+0.119$T_{mean}$+0.157SD-0.027$RH_{mean}$ |
| | MLRM 2 | FAO-56 PM ETo = 1.188+0.332$U_{mean}$+0.048$T_{mean}$+0.137SD-0.024$RH_{mean}$+0.069$T_{max}$ |
| Tongyoung | MLRM 1 | FAO-56 PM ETo = 1.356+0.094$U_{mean}$+0.134$T_{mean}$+0.160SD-0.024$RH_{mean}$ |
| | MLRM 2 | FAO-56 PM ETo = 1.646+0.076$U_{mean}$+0.182$T_{mean}$+0.169SD-0.025$RH_{mean}$ -0.049$T_{max}$ |

Table 11. Equations of MLRM 1 and MLRM 2 calculated by the training data

It is worthwhile to compare the relative importance of the variables as indicated by the indendent variables correlations. Table 12 shows the correlation matrix of FAO-56 ETo data base for MLRM 2 of Daegu station. In Daegu station, the indendent variables correlations for MLRM 2 indicate that $T_{max}$ is the most important (R=0.820), with $T_{mean}$ and SD being less important (R=0.760 & R=0.522). $RH_{mean}$ is more important $U_{mean}$ (R=-0.169 vs 0.031). In this study, from the results of correlation matrix for MLRM 1 and MLRM 2 of 8 meteorological stations, $T_{mean}$ (MLRM 1) and $T_{max}$ (MLRM 2) are the most important independent variables, respectively.

| Variable | $X_1$ | $X_2$ | $X_3$ | $X_4$ | $X_5$ | Y |
|---|---|---|---|---|---|---|
| mean wind speed | 1.000 | -0.245 | 0.168 | -0.327 | -0.287 | 0.031 |
| mean temperature | | 1.000 | -0.024 | 0.426 | 0.982 | 0.760 |
| sunshine duration | | | 1.000 | -0.667 | 0.105 | 0.522 |
| mean relative humidity | | | | 1.000 | 0.330 | -0.169 |
| max temperature | | | | | 1.000 | 0.820 |
| FAO-56 ETo | | | | | | 1.000 |

Table 12. Correlation matrix of FAO-56 ETo data base for MLRM 2 of Daegu station

MLRM 1 and MLRM 2 were validated by the testing data of MLP-NNM and SVM-NNM. Table 13 shows statistics results of MLRM 1 and MLRM 2 calculated by the testing data for Daegu, Ulsan, Jeonju, and Tongyoung stations, respectively. We could consider that the performance of MLP-NNM and SVM-NNM was better than that of MLRM 1 and MLRM 2.

| Station | Model | CC | RMSE (mm/day) | $R^2$ |
|---|---|---|---|---|
| Daegu | MLRM 1 | 0.952 | 0.562 | 0.899 |
| | MLRM 2 | 0.952 | 0.561 | 0.900 |
| Ulsan | MLRM 1 | 0.932 | 0.503 | 0.869 |
| | MLRM 2 | 0.930 | 0.510 | 0.865 |
| Jeonju | MLRM 1 | 0.934 | 0.530 | 0.863 |
| | MLRM 2 | 0.938 | 0.514 | 0.871 |
| Tongyoung | MLRM 1 | 0.908 | 0.567 | 0.824 |
| | MLRM 2 | 0.908 | 0.568 | 0.823 |

Table 13. Statistics results of MLRM 1 and MLRM 2 calculated by the testing data

## 6. Conclusions

Neural networks model provides a quick and flexible means for modeling of many hydrological processes and has showed better performance than the conventional methods. The hydrologic system under study may be nonlinear and multivariate, and the variables may have unknown interrelationships. Such problems can be efficiently explained by the neural networks model.

In this study, the potential of MLP-NNM and SVM-NNM for the modeling of FAO-56 PM ETo using climatic data has been illustrated. The study demonstrated that the modeling of FAO-56 PM ETo is possible through the use of MLP-NNM and SVM-NNM technique. For 8

meteorological stations which were selected for this study, there are no observed data for the ETo. The data calculated using FAO-56 PM ETo can be assumed as the observed ETo, whose reliability was verified by many previous studies. The following conclusions could be drawn from this study.

1. MLP 4, whose inputs are mean wind speed ($U_{mean}$), mean temperature ($T_{mean}$), sunshine duration (SD), and mean relative humidity ($RH_{mean}$) was found to perform the best among the input combinations for Seoul, Seongsanpo, Ulsan, and Hanam stations. And, MLP 5, whose input are mean wind speed ($U_{mean}$), mean temperature ($T_{mean}$), sunshine duration (SD), mean relative humidity ($RH_{mean}$), and max temperature ($T_{max}$) was found to perform the best among the input combinations for Gunsan, Daegu, Jeonju, and Tongyoung stations.
2. SVM 5, whose input are mean wind speed ($U_{mean}$), mean temperature ($T_{mean}$), sunshine duration (SD), mean relative humidity ($RH_{mean}$), and max temperature ($T_{max}$) was found to perform the best among the input combinations for 8 meteorological stations. This indicates that all these variables are needed for the better modeling of FAO-56 PM ETo using SVM-NNM.
3. The temperature, sunshine duration, and relative humidity were found to be more effective than the wind speed in the modeling of FAO-56 PM ETo.
4. The performance statistics results of SVM-NNM were better than those of MLP-NNM. It can obviously be seen from CC, RMSE, and $R^2$ statistics.
5. The potential of MLP-NNM and SVM-NNM were tested using MLRM 1 and MLRM 2. From the statistics results, the performance of MLP-NNM and SVM-NNM was better than that of MLRM 1 and MLRM 2.

MLP-NNM and SVM-NNM could be of use in water buget of watersheds and various other hydrological analysis where other models may be inappropriate. This study used only a single crop, grass reference crop, for a limited period and further studies using different crop such as alfalfa and rice reference crop may be required to strengthen these conclusions. FAO-56 PM ETo, furthermore, includes some errors in the estimation of many climatic variables. Because the ET are relatively important for the design of irrigation facilities and agricultural reservoirs, the spread of automatic measuring systems for the ET is important and urgent to ensure the reliable and accurate data from the measurements of ET, Republic of Korea.

## 7. References

Allen, R.G.; Jensen, M.E.; Wright, J.L. & Burman, R.D. (1989). Operational estimates of reference evapotranspiration. *Agronomy Journal*, Vol. 81, No. 4, pp. 650-662, ISSN: 0002-1962.

Allen, R.G.; Pereira, L.S.; Raes, D. & Smith, M. (1998). *Crop evapotranspiration. Guidelines for computing crop water requirement*, Irrigation and Drainage Paper No. 56, FAO, Rome, Italy.

ASCE Task Committee on Application of Neural Networks in Hydrology. (2000). Artificial Neural Networks in Hydrology. Ⅰ: Preliminary concepts. *Journal of Hydrologic Engineering, ASCE*, Vol. 5, No. 2, pp. 115-123, ISSN: 1084-0699.

ASCE Task Committee on Definition of Criteria for Evaluation of Watershed Models. (1993). Criteria for evaluation of watershed models. *Journal of Irrigation and Drainage Engineering, ASCE*, Vol. 119, No. 3, pp. 429-442, ISSN: 0733-9437.

Bishop, C.M. (1994). Neural networks and their applications. *Review of Scientific Instruments*, Vol. 65, pp. 1803-1832, ISSN: 0034-6748.

Bishop, C.M. (1995). *Neural networks for pattern recognition*, Oxford University Press, ISBN: 0198538642, NY, USA.

Brutsaert, W.H. (1982). *Evaporation into the atmosphere*, Springer-Verlag, ISBN: 9027712476, NY, USA.

Chang, C.C & Lin, C. (2001). *LIBSVM : a library for support vector machines*, Software avaliable http://www.csie.ntu.edu.tw/cjlin/libsvm.

Cover, T.M. (1965). Geometrical and statistical properties of systems of linear inequalities with applications in pattern recognition. *IEEE Transactions on Electronic Computers EC-14*, pp. 326-334.

Dibike, Y.B.; Velickov, S.; Solomatine, D. & Abbott, M.B. (2001). Model induction with support vector machines: introductions and applications. *Journal of Computing in Civil Engineering*, *ASCE*, Vol. 15, No. 3, pp. 208-216, ISSN: 0887-3801.

Doorenbos, J. & Pruitt, W.O. (1977). *Guidelines for predicting crop water requirement*, Irrigation and Drainage Paper No. 24 2nd Edition, FAO, Rome, Italy.

Haykin, S. (2009). *Neural networks and learning machines 3rd Edition*, Prentice Hall, ISBN: 0131471392, NJ, USA.

Hush, D.R. & Horne, B.G. (1993). Progress in supervised neural network : What's new since Lippmann ?. *IEEE Signal Processing Magazine*, Vol. 10, pp. 8-39, ISSN: 1053-5888.

Jain, S.K.; Nayak, P.C. & Sudheer, K.P. (2008). Models for estimating evapotranspiration using artificial neural networks, and their physical interpretation. *Hydrological Processes*, Vol. 22, pp. 2225-2234, ISSN: 0885-6087.

Jensen, M.E.; Burman, R.D. & Allen, R.G. (1990). *Evapotranspiration and irrigation water requirements*, ASCE Manual and Report on Engineering Practice No. 70, ASCE, NY, USA.

Gallant, S.I. (1993). *Neural Network learning and expert system*, MIT Press, ISBN: 0262071452, MA, USA.

Khadam, I.M. & Kaluarachchi, J.J. (2004). Use of soft information to describe the relative uncertainty of calibration data in hydrologic models. *Water Resources Research*, Vol. 40, No. 11, W11505, ISSN: 0043-1397.

Khoob, A.R. (2008a). Comparative study of Hargreaves's and artificial neural network's methodologies in estimating reference evapotranspiration in a semiarid environment. *Irrigation Science*, Vol. 26, No. 3, pp. 253-259, ISSN: 0342-7188.

Khoob, A.R. (2008b). Artificial neural network estimation of reference evapotranspiration from pan evaporation in a semi-arid environment. *Irrigation Science*, Vol. 27, No. 1, pp. 35-39, ISSN: 0342-7188.

Kim, S. (2004). Neural Networks Model and Embedded Stochastic Processes for Hydrological Analysis in South Korea. *KSCE Journal of Civil Engineering*, Vol. 8, No. 1, pp. 141-148, ISSN: 1226-7988.

Kim, S.; Kim, J.H. & Park, K.B. (2009). Neural Networks Models for the Flood Forecasting and Disaster Prevention System in the Small Catchment. *Disaster Advances*, Vol. 2, No. 3, pp. 51-63, ISSN: 0974-262X.

Kim, S. & Kim, H.S. (2008). Neural networks and genetic algorithm approach for nonlinear evaporation and evapotranspiration modeling. *Journal of Hydrology*, Vol. 351, pp. 299-317, ISSN: 0022-1694.

Kish, O. (2006). Generalized regression neural networks for evapotranspiration modeling. *Hydrological Sciences Journal*, Vol. 51, No. 6, pp. 1092-1105, ISSN: 0262-6667.

Kish, O. (2007). Evapotranspiration modeling from climatic data using a neural computing technique. *Hydrological Processes*, Vol. 21, pp. 1925-1934, ISSN: 0885-6087.

Kish, O. (2008). The potential of different ANN techniques in evapotranspiration modeling. *Hydrological Processes*, Vol. 22 , pp. 2449-2460, ISSN: 0885-6087.

Kisi, O. & Ozturk, O. (2007). Adaptive neurofuzzy computing technique for evapotranspiration estimation. *Journal of Irrigation and Drainage Engineering, ASCE*, Vol. 133, No. 4, pp. 368-379, ISSN: 0733-9437.

Kottegoda, N.T. (1998). *Statistics, probability, and reliability for civil and environmental engineers*, McGraw-Hill, ISBN: 0070359652, Singapore.

Kumar, M.; Bandyopadhyay, A.; Raghuwanshi, N.S. & Singh, R. (2008). Comparative study of conventional and artificial neural network-based ETo estimation models. *Irrigation Science*, Vol. 26, No. 6, pp. 531-545, ISSN: 0342-7188.

Kumar, M.; Raghuwanshi, N.S. & Singh, R. (2009). Development and validation of GANN model for evapotranspiration estimation. *Journal of Hydrologic Engineering, ASCE*, Vol. 14, No. 2, pp. 131-140, ISSN: 1084-0699.

Kumar, M.; Raghuwanshi, N.S.; Singh, R.; Wallender, W.W. & Pruitt, W.O. (2002). Estimating evapotranspiration using artificial neural network. *Journal of Irrigation and Drainage Engineering, ASCE*, Vol. 128, No. 4, pp. 224-233, ISSN: 0733-9437.

Landeras, G.; Barredo, A.O. & Lopez, J.J. (2008). Comparison of artificial neural network models and empirical and semi-empirical equations for daily reference evapotranspiration estimation in the Basque country (Northern Spain). *Agricultural Water Management*, Vol. 95, No. 5, pp. 553-565, ISSN: 0378-3774.

McCuen, R.H. (1993). *Microcomputer applications in statistical hydrology*, Prentice Hall, ISBN: 0135852900, Englewood Cliffs, NJ, USA.

Monteith, J.L. (1965). The state and movement of water in living organism, *Proceedings of Evaporation and Environment*, pp. 205-234, Swansea, Cambridge University Press, NY, USA.

Nash, J.E. & Sutcliffe, J.V. (1970). River flow forecasting through conceptual models, Part 1 - A discussion of principles. *Journal of Hydrology*, Vol. 10, No. 3, pp. 282-290, ISSN: 0022-1694.

Penman, H.L. (1948). Natural evaporation from open water, bare soil and grass, *Proceedings of the Royal Society of London*, Vol. 193, pp. 120-146, London, England.

Principe, J.C.; Euliano, N.R. & Lefebvre, W.C. (2000). *Neural and adaptive systems: fundamentals through simulation*, Wiley, John & Sons, ISBN: 0471351679, NY, USA.

Salas, J.D.; Smith, R.A., Tabios Ⅲ, G.O. & Heo, J.H. (2001). *Statistical computing techniques in water resources and environmental engineering*, Unpublished book in CE622, Colorado State University, Fort Collins, CO, USA.

Simpson, P.K. (1990). *Artificial neural systems: foundations, paradigms, applications and implementations*, Elsevier, ISBN: 0080378943, NY, USA.

Singh, V.P. (1988). *Hydrologic system rainfall-runoff modeling. Vol. 1*, Prentice Hall, ISBN: 0134480511, NJ, USA.

Specht, D.F. (1991). A general regression neural network. *IEEE Transactions on Neural Networks*, Vol. 2 No. 6, pp. 568-576, ISSN: 1045-9227.

Sudheer, K.P.; Gosain, A.K. & Ramasastri, K.S. (2003). Estimating actual evapotranspiration from limited climatic data using neural computing technique. *Journal of Irrigation and Drainage Engineering, ASCE*, Vol. 129, No. 3, pp. 214-218, ISSN: 0733-9437.

Traore, S.; Wang, Y.M. & Kerh, T. (2010). Artificial neural network for modeling reference evapotranspiration complex process in Sudano-Sahelian zone. *Agricultural Water Management*, Vol. 97, No. 5, pp. 707-714, ISSN: 0378-3774.

Trajkovic, S. (2005). Temperature-based approaches for estimating reference evapotranspiration. *Journal of Irrigation and Drainage Engineering, ASCE*, Vol. 131, No. 4, pp. 316-323, ISSN: 0733-9437.

Trajkovic, S; Todorovic, B. & Stankovic, M. (2003). Forecasting reference evapotranspiration by artificial neural networks. *Journal of Irrigation and Drainage Engineering, ASCE*, Vol. 129, No. 6, pp. 454-457, ISSN: 0733-9437.

Tripathi, S.; Srinivas, V.V. & Nanjundish, R.S. (2006). Downscaling of precipitation for climate change scenarios: A support vector machine approach. *Journal of Hydrology* , Vol. 330, pp. 621-640, ISSN: 0022-1694.

Tsoukalas, L.H. & Uhrig, R.E. (1997). *Fuzzy and Neural Approaches in Engineering*, Wiley, John & Sons, ISBN: 0471192473, NY, USA.

Vapnik, V.N. (1992). Principles of risk minimization for learning theory. In: *Advances in Neural Information Processing Systems Vol. 4*, Moody, Hanson & Lippmann, (Ed.), pp. 831-838, Elsevier, ISBN: 1558602224, NY, USA.

Vapnik, V.N. (2010). *The nature of statistical learning theory 2nd Edition*, Springer-Verlag, ISBN: 0387987800, NY, USA.

Wasserman, P.D. (1993). *Advanced methods in neural computing*, Wiley, John & Sons, ISBN: 0442004613, NY, USA.

Zanetti, S.S.; Sousa, E.F.; Oliveira, V.P.S.; Almeida, F.T. & Bernardo, S. (2007). Estimating evapotranspiration using artificial neural network and minimum climatological data. *Journal of Irrigation and Drainage Engineering, ASCE*, Vol. 133, No. 2, pp. 83-89, ISSN: 0733-9437.

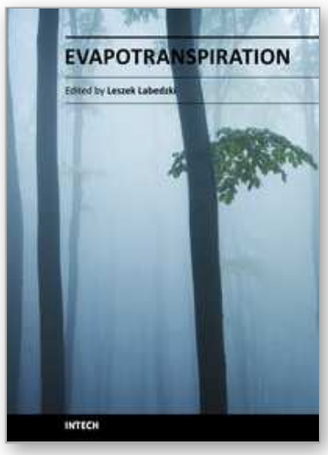


**Evapotranspiration**

Edited by Prof. Leszek Labedzki

ISBN 978-953-307-251-7
Hard cover, 446 pages
**Publisher** InTech
**Published online** 16, March, 2011
**Published in print edition** March, 2011

Evapotranspiration is a very complex phenomenon, comprising different aspects and processes (hydrological, meteorological, physiological, soil, plant and others). Farmers, agriculture advisers, extension services, hydrologists, agrometeorologists, water management specialists and many others are facing the problem of evapotranspiration. This book is dedicated to further understanding of the evapotranspiration problems, presenting a broad body of experience, by reporting different views of the authors and the results of their studies. It covers aspects from understandings and concepts of evapotranspiration, through methodology of calculating and measuring, to applications in different fields, in which evapotranspiration is an important factor. The book will be of benefit to scientists, engineers and managers involved in problems related to meteorology, climatology, hydrology, geography, agronomy and agricultural water management. We hope they will find useful material in this collection of papers.



INTECH
open science | open minds

**InTech Europe**
University Campus STeP Ri
Slavka Krautzeka 83/A
51000 Rijeka, Croatia
Phone: +385 (51) 770 447
Fax: +385 (51) 686 166
www.intechopen.com

**InTech China**
Unit 405, Office Block, Hotel Equatorial Shanghai
No.65, Yan An Road (West), Shanghai, 200040, China
中国上海市延安西路65号上海国际贵都大饭店办公楼405单元
Phone: +86-21-62489820
Fax: +86-21-62489821

IntechOpen